DELAMINATION GROWTH AND FIBRE/MATRIX PROGRESSIVE DAMAGE IN COMPOSITE PLATES UNDER COMPRESSION

Elisa Pietropaoli[1] , Aniello Riccio[1] and Mauro Zarrelli[2]

[1]C.I.R.A Italian Aerospace Research Center
Computational Mechanics Laboratory
via Maiorise 81043 Capua,Italy
e.pietropaoli@cira.it
a.riccio@cira.it

[2]CNR IMCB
Institute for Composite and Biomedical Materials
National Research Council
Piazzale Enrico Fermi, 80055 Portici,Italy
mauro.zarrelli@imcb.cnr.it

ABSTRACT

The behaviour of delaminated composite plates under compressive load has been investigated by means of a numerical procedure implemented in the B2000 FEM code. In this work the widely studied delamination growth phenomena in composite plates under compression has been investigated by taking into account also the matrix and fibres breakages until the structural collapse condition is reached.
The delamination growth has been simulated by means of interface elements based on the modified virtual crack closure technique (MVCCT) to evaluate the Strain energy Release Rate. Furthermore, an iterative numerical procedure has been introduced to simulate the progressive matrix and fibre breakage by adopting respectively the Hashin's failure criteria to check the stress state and instantaneous degradation rules for the reduction of the damaged material properties. The penalty method approach has been used for the formulation of the contact phenomena whose introduction in the model is demonstrated to be mandatory when a compressive load is applied to the structure.
The developed procedure has been applied for analysing the mechanical behaviour under compression of a delaminated composite plate. The obtained buckling and post-buckling responses have been compared with experimental data on composite coupons with embedded delaminations.

1. INTRODUCTION

The mechanical behaviour of post-buckled composite structures is governed by the onset, evolution and interaction of interlaminar (delaminations) and intralaminar (fiber/matrix failures) damages.
Analyses on impacted CFRP always shown the simultaneous presence of matrix failures and delaminations. Therefore it is reasonable to assume that an accurate prediction of the residual stiffness and strength of delaminated structures under compressive loads, requires that intralaminar damages must be taken into account.
A great amount of literature works are devoted to the numerical analysis of the post-buckling behaviour of embedded delamination [1-7] but only in a few cases intralaminar damages have been simultaneously considered too [8-11].
Finite element procedures dealing with the delamination growth are based on fracture mechanics concepts and usually involve the evaluation of the Strain Energy Release Rates (ERR) at the delamination front. Rough approaches do not take into account the modes separation and evaluate only a total value of the ERR[9] while more sophisticated techniques such as the Virtual Crack Closure Technique(VCCT) [12]

allow to compute the ERRs for the three basic fracture modes (G_I,G_{II} and G_{III}) starting from nodal forces and displacement computed at the delamination front.
Furthermore it is assumed that when a prescribed function of the computed ERRs overcomes a threshold value dependent on the fracture toughness of the material (G_{Ic},G_{IIc} and G_{IIIc} or Gc), the delamination front is modified thus simulating the delamination opening.
The modification of delamination front can be obtained by a moving mesh method as proposed in Ref.[8,9] or by releasing not merged nodes laying in the same position but belonging to two different fracture surfaces [4,10,11].
When dealing with delaminated structures, overlaps can be induced between the de-bonded layers, therefore contact elements must be used to obtain meaningful results[2-,3]. The introduction of these element enhance the agreement of the numerical results with respect to the experimental ones but induces numerical convergence problems thus requiring a very stable nonlinear solver.
Concerning the intralaminar damages, different failure criteria are available in literature for the individuation of the first ply failure load such as the Hashin's criteria[13-15] whose peculiar characteristic is that they allow to distinguish among different failure modes.
It is well known that composite plates retain residual stiffness and strength after the occurrence of the first ply failure. A widely used approach for the simulation of the behaviour of composite structures beyond the detection of the first ply failure, consists in a change of the material properties for failed elements according to suitable degradation rules. This approach has been extensively utilised for the analysis of composite plates with holes [16-23] but only in a few cases has been applied to the analysis of delaminated plates [9,11].
The numerical simulation of the compression after impact behaviour of composite plates requires that all these features (evaluation of the ERRs, failure check and degradation approach) be included into an iterative non linear procedure.
In this paper the post-buckling behaviour of a composite plate with an embedded delamination has been analysed by using this multifaceted procedure that has been implemented in the B2000 finite element code. The comparison with experimental results [8] is provided, putting evidence on delamination growth and fiber/matrix failures.

1. PROBLEM FORMULATION

The stiffness and strength reduction associated to the presence of a delamination in a composite laminate plates is very strong especially in compression.
The experimental measure of residual properties of impact-damaged structures usually foresees the presence of an artificial delamination obtained by placing a very thin film of Teflon between two adjacent layer of a composite laminate. The laminate is thus subdivided into a thin sub-laminate and a thick sublaminate or base sublaminate.
Two edges of the plate are then clamped in a test machine and a compressive displacement is gradually applied. The behaviour of the damaged plates can be defined by monitoring the out of plane displacement of the two sublaminates.
A schematic description of the feasible configurations that can be encountered for this type of test is given in Figure 1.
As the load increases the thin sublaminate buckles first (see Figure 1 (b)). Afterwards, the buckling of the base sublaminate is induced (global-buckling). In this case, depending on the thicknesses ratio of the two sub-laminates, the out of plane

displacement of the base sublaminate can be of the same sign (Figure 1 (c)-Type II) or of different sign (Figure 1 (c)-Type I) with respect to the one of the thin sub-laminate. When the global buckling is of Type II, an increase in applied load determines the condition known as mixed buckling: the thin sublaminate is dragged towards the base sublaminate but the delamination opening continues to be relevant (see Figure 1 (d)).

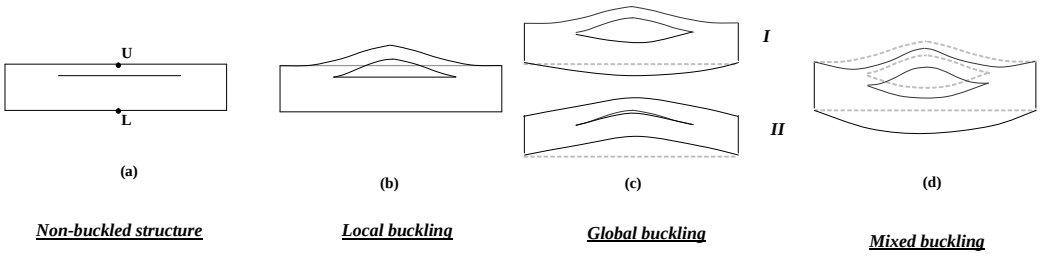

Figure 1: Delamination buckling modes

The delamination starts to growth generally after the global buckling but a delamination propagation after the local buckling could be also possible for different constraints or delamination shapes depending on the stress distribution at the delamination front.
In the same way, intralaminar damages, depending on the stress state within the material can be induced before or after the delamination growth.

2. FINITE ELEMENT MODELLIZATION

In order to simulate numerically the phenomenology described in Section 1 several aspects need to be considered. In particular the presence of an embedded delamination that can growth and the need to know the three dimensional stress state within the material (from which depends both the occurrence of intralaminar damages and the progression of the delamination front) must be managed.
In this work the structure has been discretized by means of 20 nodes layered isoparametric elements that allow to compute also interlaminar shearing stresses τ_{xz}, τ_{yz} and the normal stress σ_{zz}. The delamination is simulating by maintaining not merged nodes on two adjacent faces of the volumes representing respectively the thin and the base sublaminate.
The simulation of the delamination growth is performed by evaluating the Energy Release Rate at the delamination front by means of the Modified Virtual Crack Closure Technique [3,4,7,11,12]: displacement and forces at the delamination front are evaluated at the nodes of interface fracture elements [4,10,11] placed on the delamination surface (Zone II of Figure 2). Within these elements, nodes belonging to the delamination front are keeping together (Figure 2 (a)) until the overcoming of a threshold value for the energy release rate (see Eq.1), after, the propagation of the delamination front is obtained by disconnecting these nodes (Figure 2 (b)).

$$Ed = \left(\frac{G_I}{G_{I\,C}}\right) + \left(\frac{G_{II}}{G_{II\,C}}\right) + \left(\frac{G_{III}}{G_{III\,C}}\right) \geq 1 \qquad (1)$$

Three dimensional node to node contact elements, based on the penalty formulation [3], have been placed in the delamination zone (Zone I and II of Figure 2) to avoid overlaps between the two sublaminates.

Once the finite element model is available, a classical non-linear static analysis is performed following the non-linear incremental approach proposed by Riks [25] available in B2000.

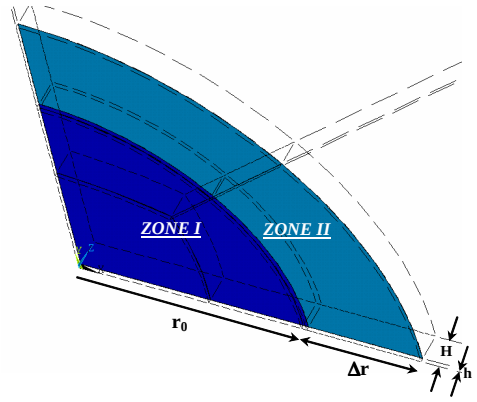

Figure 2: Initial delamination area (radius r_0 -ZONE I) and area where the delamination is expected to grow (Δr-ZONEII) .

In Figure 3 the flowchart of the Progressive Damage –Delamination Growth finite element procedure developed for the simulation of interaction and evolution of intralaminar and interlaminar damages is shown.

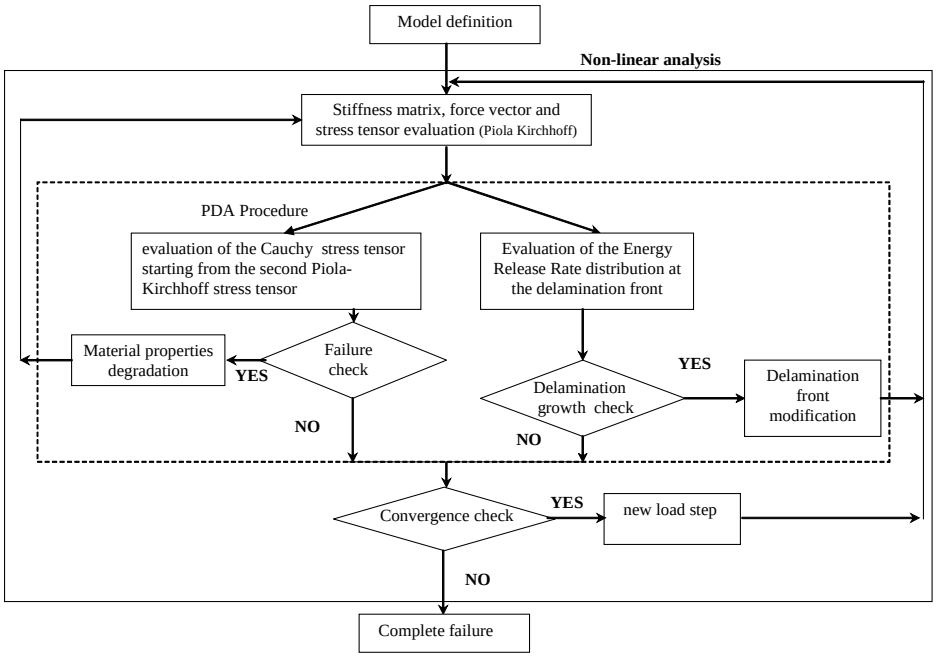

Figure 3: Progressive damage-delamination growth procedure flow chart

The discretization the structure in a finite number of elements allows to select a reduced number of points (namely the integration points) where the intralaminar failure check (Hashin's failure criteria [13-15]) have to be executed. It should be noted that the occurrence of matrix cracks, fibre breakages and all the other intralaminar damages are verified for each ply of the laminate. In order to take into account the evidence that a failure in single ply could not induce the collapse of the entire element, only the

material properties of the damaged ply of the finite element under consideration are reduced according to suitable degradation rules [16-23] depending on the failure mode detected. The three dimensional stress state within the material has influence on the onset and evolution of intralaminar failures but also on the delamination growth. A check on the Energy Release Rate at the delamination front is performed within each load step and eventually the delamination front is modified by releasing nodes of interface fracture elements.
The simultaneous analysis of delamination growth and intralaminar damages allows to take into account effects of the stress redistribution induced by intralaminar damages on the speed of the delamination front propagation and conversely to analyse intralaminar damages arisen from stress concentrations associated to the delamination growth.

3. FINITE ELEMENT ANALYSIS: COMPRESSION AFTER IMPACT OF A DELAMINATED COMPOSITE PLATES

The procedure described in section 2 has been used in order to compute the post-impact residual stiffness and strength for the composite plate analysed by Nilsson,Asp and Sjogren in Ref.8. The geometry of the benchmark and the material properties are given respectively in Figure 4 and Table 1.

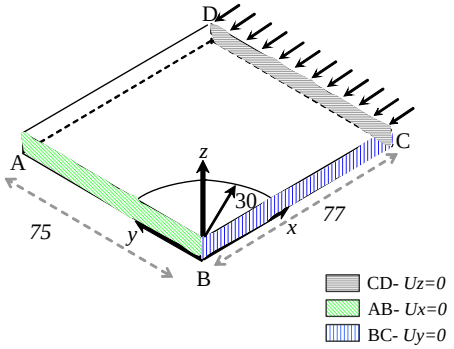

Figure 4: Benchmark geometry and applied boundary conditions

As suggested in Ref.8 with respect of the real dimensions of the specimen an increased "apparent" panel length of 77mm and a reduced thickness (equal to 3.96 mm instead of 4.16 mm) have been assumed. The stacking sequence for the laminate is: $[90/-45/+45/0_2/+45/-45/90/0/+45/-45/90_2/-45/+45/0]_2$ with a delamination placed at the 27th ply-interface (-45/90).

Material ply thickness	t	*0.13 mm*
Longitudinal Young's Modulus	E_{11}	*131 GPa*
Transverse Young's Modulus	E_{22}	*11.7 GPa*
Shear Modulus	$G_{12}=G_{13}$	*5.25 GPa*
	G_{23}	*3.9 GPa*
Poisson's Ratio	$\nu_{12}= \nu_{13}$	*0.3*
	ν_{23}	*0.51*
Longitudinal tensile strength	X_T	*1500 MPa*
Transverse tensile strength	Y_T	*40 MPa*
Longitudinal compression strength	X_C	*1500 MPa*
Transverse compression strength	Y_C	*246 MPa*
In-plane shear strenght	S	*68 MPa*
Critical strain energy release rate for mode I	G_{IC}	*250 J/m^2*
Critical strain energy release rate for mode II	G_{IIC}	*820 J/m^2*

Table 1: Material Properties for the HTA/6376C [8] (The strengths are not characterized experimentally. Typical values for carbon/epoxy laminate have been assumed)

In Figure 4 are also indicated the boundary conditions applied: it should be noted that only one quarter of the structures has been analysed for symmetry considerations. The clamping of the test tabs at the edges of the plate has been simulated by imposing that the out of plane displacement on this edges has to be zero. Only conditions on displacements have been imposed because the volume has been meshed by using solid elements.
Three different approaches have been used in what follows:

BASE model: the simulation is carried on without considering intralaminar damages and delamination growth.
DEL model: only the delamination growth is taken into account
PDADEL model: both delamination growth and intralaminar damages are considered and the complete procedure shown in Figure 3 is used.

The comparison of the results given from these approaches allows to put evidence on effects respectively of delamination growth and intralaminar damages on the global response of the structures.

Results will be given in term of out of plane displacement versus applied load graphs, energy release rate distributions at the moving delamination front and failure maps showing with a scale of colour different typologies of damage.

3.1 Comparison with experimental results.

The structural response in term of out of plane displacement versus applied load and displacement obtained with the three proposed approaches BASE,DEL,PDADEL is shown in Figure 5 and Figure 6. A good agreement with experimental results available in Ref.8 has been found in term of local and global buckling loads.
The delamination growth initiation it is also well predicted (see Table 3) but an overestimation of the out of plane displacements of the two sublaminates it is also evident before failure (see Figure 5) more for the DEL approach that for the PDADEL.

	$P_{growth}/2$ (KN)	$\delta_{growth}/2$ (mm)
Plate 1_1 [8]	32.5	0.185
Plate 2_1 [8]	34	0.225
Plate 3_1 [8]	34.5	0.215
PDADEL	32.96	0.175

Table3: Delamination growth initiation

Differences between BASE,DEL and PDADEL curves allow to highlight the role, respectively of delamination growth and intralaminar onset and evolution, on the overall structural behaviour. It is worth noting that the slope variation of the curves DEL and PDADEL with respect to the BASE one, noticeable after the global buckling (Figure 5 and Figure 6), is due to the start of the delamination growth (Table 3). Besides the comparison between the out of plane displacements of the thin and the base sublaminate at the collapse point obtained by the PDADEL and DEL approaches puts evidence on the stiffness reduction associated to the onset of intralaminar damages.

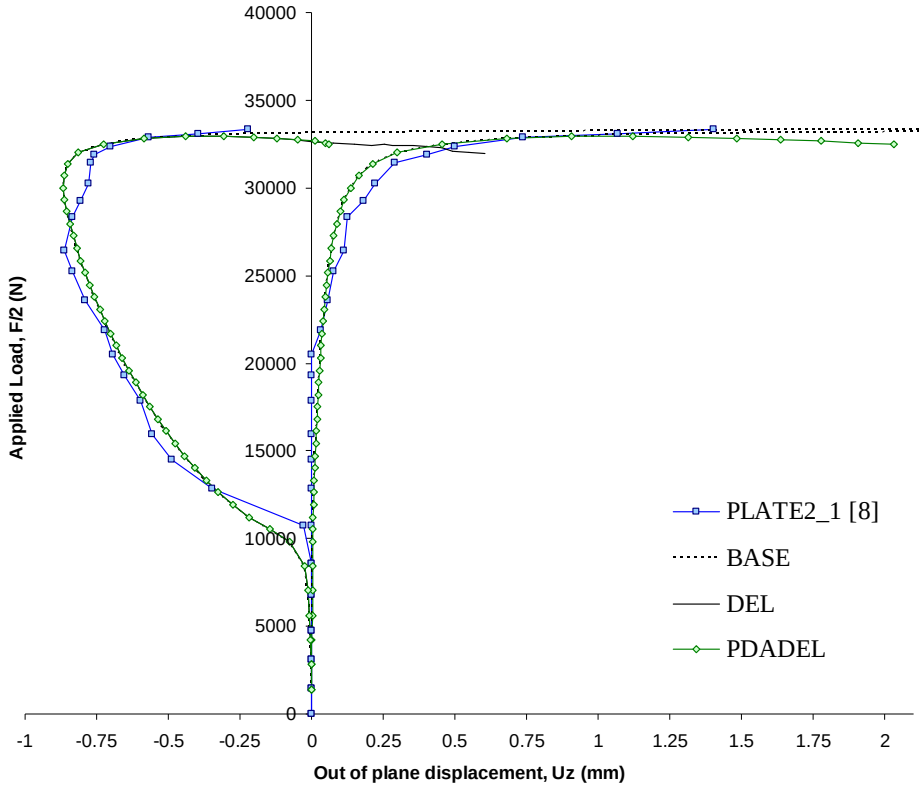

Figure 5: Out of plane displacement versus applied load

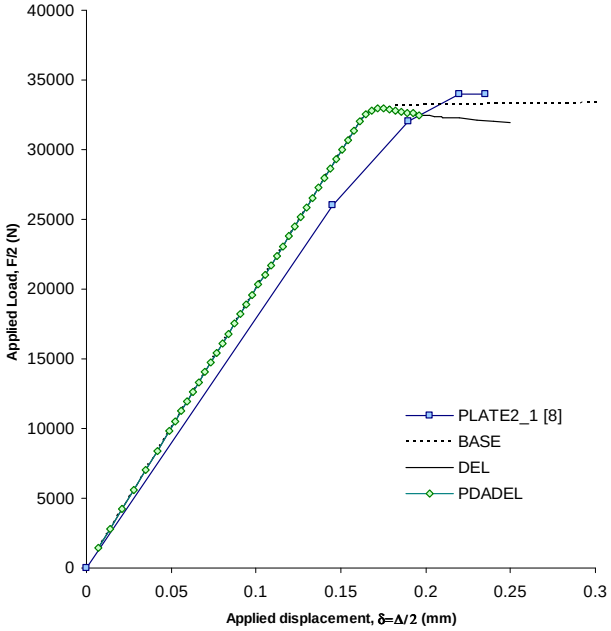

Figure 6: Applied displacement versus applied load

The propagation of the delamination front induced by an increase in applied load is shown in Figure 7.

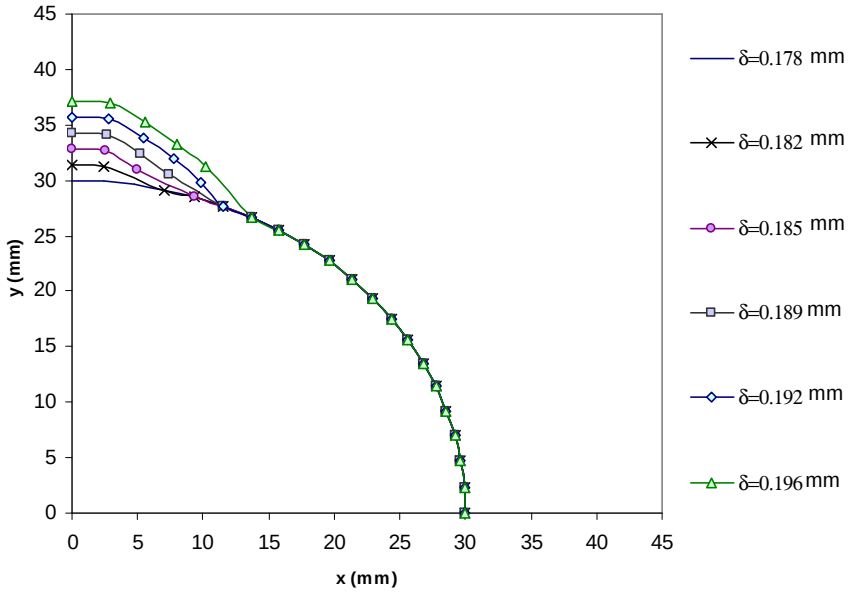

Figure 7: Delamination front at different applied loads.

The Energy Threshold level distribution at the delamination front (eq .1) is given in Figure 8 showing how an increase in load induces a progressively increase of Ed until the overcoming of the value 1 will produce the propagation of the delamination front (Figure 7 and Figure 8).

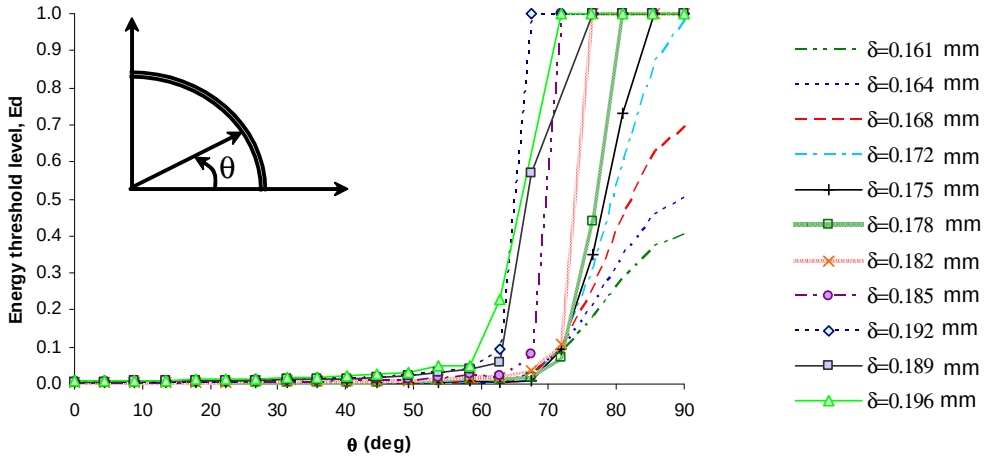

Figure 8: Threshold energy level at different applied loads (before and after the start of the delamination growth.

The delamination growth is driven by the first of the three basic fracture modes as it can be seen from Figure 9 where it is evident that the ratio G_I/G_{Ic} is greater than G_{II}/G_{IIc}.

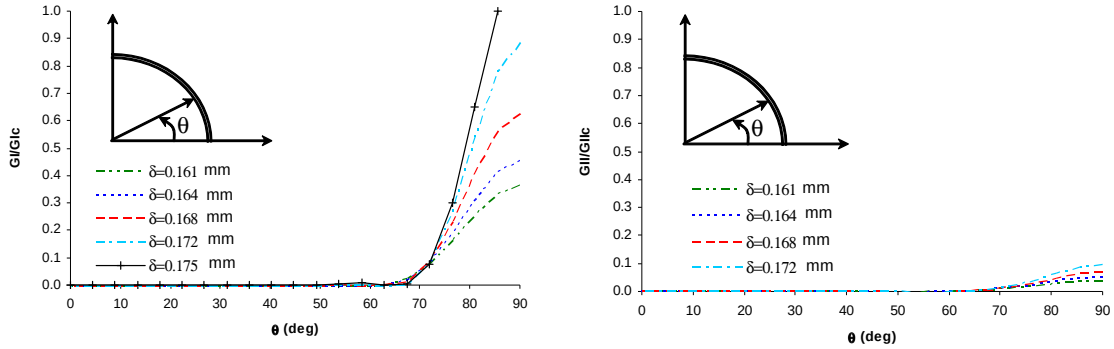

Figure 9:Energy release rate at the delamination front before the delamination growth.

The failure maps obtained by using the PDADEL approaches are shown for the first (0°) (Figure 10) and the fifth (90°) (Figure 11) ply of the thin sublaminate where the load is acting perpendicularly to the delamination opening. In these figures the colour map is related to different failure modes: blue for undamaged ply (0-2), green for matrix failures (5) , yellow for fibre failures (8) and red for completely failed ply 11.
At early stages only matrix failures within the initial extension of the delamination appear, after, as the load increases and the delamination propagates more, the damaged area increases and fibre breakages come out too.

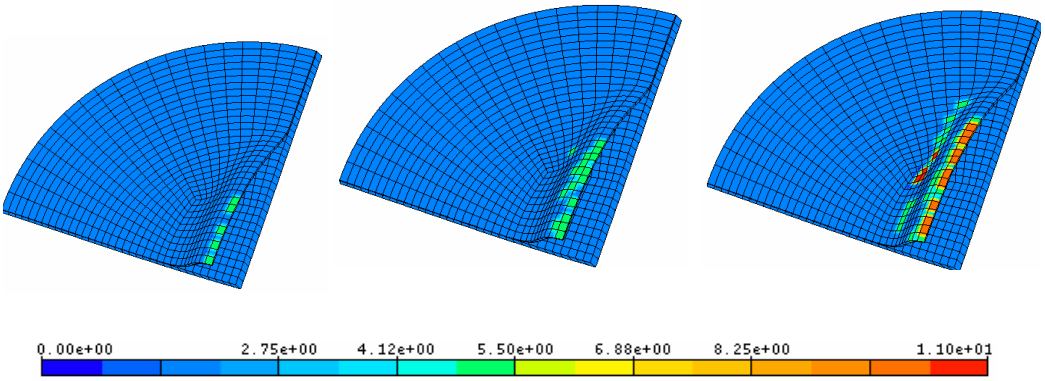

Figure 10: Failure maps for the first ply of the thin sublaminate

(δ= 0.812mm, δ= 0.188 mm and δ=0.196mm)

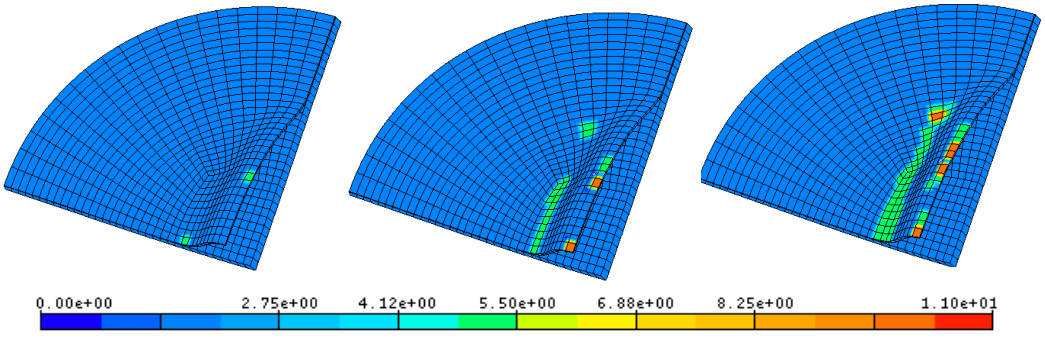

Figure 11: Failure maps for the fifth ply of the thin sublaminate

(δ= 0.812mm, δ= 0.188 mm and δ=0.196mm)

The effect of intralaminar damages on the delamination front propagation can be seen from the comparison between the G_I distribution at the delamination front obtained with DEL and PDADEL (Figure 12): the non-coincidence of the curve associated to DEL and PDADEL at δ=0.192mm means that an increase in the speed of the delamination propagation is associated to the appearance of intralaminar damages.

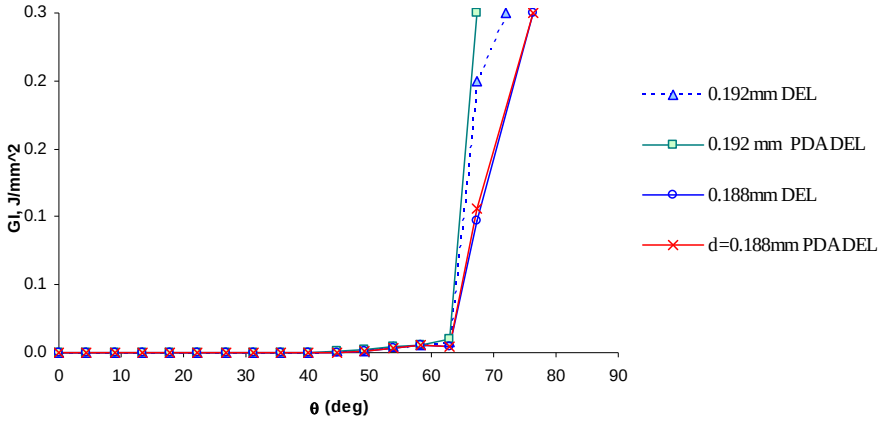

Figure 12: GI distribution at the delamination front with and without intralaminar damages.

Furthermore the comparison between stress fields obtained at δ=0.192 mm by using DEL and PDADEL (Figure 13) allows to put evidence on the stress redistribution the near the damages elements: the σ_{xx} stress for elements characterised by the presence of broken fibres (b.f.) is smaller than in undamaged adjacent elements.

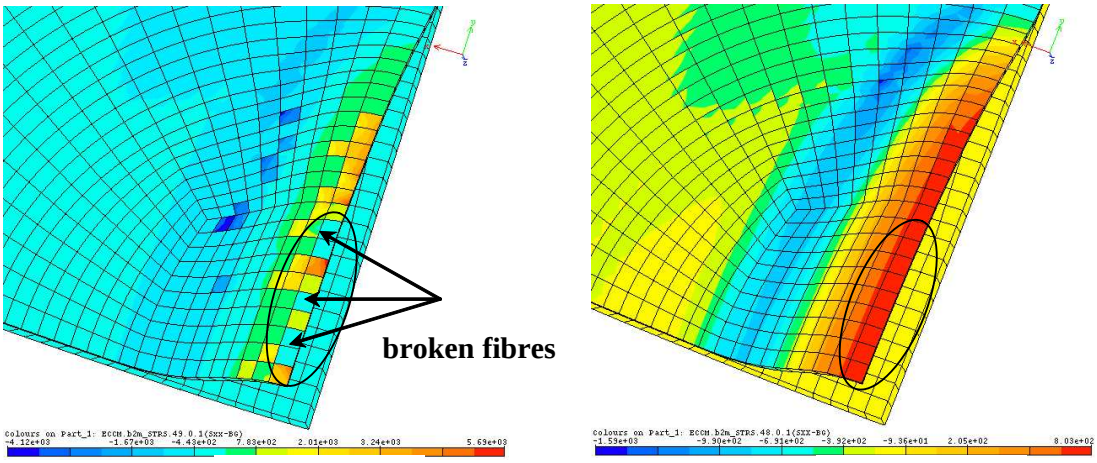

(a) **(b)**

Figure 13: Stress field σ_{xx} for the first ply of the thin sublaminate with(a) and without intralaminar damages (b). Failed elements are shown in (Figure 10-δ=0.196mm)

4. CONCLUSIONS

The post buckling behaviour of a composite plates under compressive loads has been numerically investigated by using a finite element procedure that takes into account both delamination growth and intralaminar damages onset and progression.
The MVCCT has been used for the simulation of the delamination growth by evaluating the energy release rates distribution at the delamination front for each load step of the non linear iterative analysis.
On the other hand Hashin's failure criteria and suitable material properties degradation rules have been introduced in order to simulate matrix failures and fibre breakages.
Results have been shown in term of out of plane displacement versus applied load, delamination front. A good agreement has been attained with respect to literature experimental results. Intralaminar damages have been shown by means of failure maps and their role on the overall structural behaviour has been highlighted.
It has been found that the introduction of intralaminar damages within the delamination growth analysis leads to a more accurate prediction of the collapse point of the whole structure.

ACKNOWLEDGEMENTS

The work presented in this paper has been done in collaboration with the "Seconda Università degli Studi di Napoli" (Aversa, Italy) in the frame of the doctoral thesis of Elisa Pietropaoli.

REFERENCES

1- Nilsson, K.F., Asp, L. E., Alpman J.E. and Nystedt L. "Delamination buckling and growth for delaminations at different depths in a slender composite panel". *International Journal of Solids and Structures*, 2001,38:3039-3071.
2- Whitcomb, J. D. "Analysis of a Laminate with a Postbuckled Embedded Delamination, Including Contact Effects". *Int. Journal of Composite Materials*, 1992,26:1523-1535.
3- Perugini P. , Riccio A. and Scaramuzzino F. "Influence of Delamination Growth and Contact Phenomena on the Compressive Behaviour of Composite Panels". *Int. Journal of Composite Materials*, 1999. 33(15):1433-1456.
4- Gaudenzi P. , Perugini P. and Riccio A. "Post-buckling behaviour of Composite Panels in the presence of Unstable Delaminations".*Composite Structures*, 2001,51: 301-309.
5- Whitcomb, J.D and Shivakumar K.N., "Strain-Energy Release Rate Analysis of plates with postbuckled delaminations", *Journal of Composite Materials*. 1989. 23:714-734.
6- Whitcomb, J.D "Instability related delamination growth of embedded and edge delamination", NASA/TM-1988-100655
7- Mukherjee, Y.X., Gulrajani, S.N., Mukherjee,S. and Netravali,A.N. "A numerical and experimental study of delaminated layered composites". Journal of composite materials, 1994, 28:837-870
8- Nilsson, K.F, Asp, L.E. and Sjogren, A., "On transition of delamination growth behaviour for compression loaded composite panels", International Journal of Solids and Structures, 2001,38:8407-8440

9- Sun, X., Tong L. and Chen H., “Progressive failure analysis of laminated plates with delamination”, *Journal of reinforced plastics and composites*, 2001,20: 1370-1389.
10- Liu, S. and Chang, F.K, “Matrix cracking effect on delamination growth in composite laminates induced by a spherical indenter”, *Journal of composite materials*, 1994,28:940-977
11- Riccio A. , Pietropaoli E. “Modelling damage propagation in composite plates with embedded delamination under compressive load”.2008, *Accepted for publication on Journal of Composite Materials*.
12- Krueger R. “The Virtual Crack Closure Technique: History, Approach and Applications”, NASA/CR-2002-211628
13- Hashin, Z. and Rotem, A.. “A Fatigue Failure Criterion for Fibre Reinforced Materials”, *Journal of Composite Materials*, 1973. 7:448-474.
14- Hashin, Z. “Failure Criteria for Unidirectional Fibre Composites”, *Journal of Applied Mechanics*, 1980. 47:329-334.
15- Shokrieh, M. and Lessard, L.B., “Progressive fatigue damage modeling of composite materials, Part I: modeling”, *Journal of Composite Materials*, 2000. 34:1056-1115.
16- Sleight D.W. “Progressive failure analysis methodology for laminated composite structures”, NASA/TP-1999-209107
17- Hahn, H.T. and Tsai, S.W. “On the Behaviour of Composite Laminates After Initial Failures”, *Astronautics and Aeronautics*. 1983,21:58-62.
18- Chanh Fu-Kuo and Chang Huo-Yen, “A progressive damage model for laminated composites containing stress concentrations”, *Journal of composite materials*, 1987, 21:834-855
19- Tan Seng “A Progressive failure model for composite laminates containing openings”, *Journal of Composite Materials*, 1991,25:556-577
20- Engelstad,S.P., Reddy, J.N. and Knight, N.F. “Postbuckling Response and failure prediction of Graphite-Epoxy plates loaded in compression”, AIAA Journal, 1992, 30:2106-2113
21- Hahn, H.T. and Tsai S.W., “On the behaviour of composite laminates after initiation failures”, Journal of composite materials, 1974, 8:288-305
22- Chou S-C, Orringer,O. and Rainey J.H., “Post-failure behaviour of laminates I-no stress concentration”, Journal of composite materials, 1976, 10:371-381
23- Chou S-C, Orringer,O. and Rainey J.H., “Post-failure behaviour of laminates II-stress concentration”, *Journal of composite materials*, 1977, 11:71-78
24- Hu, N., Fukunaga,H, Sekine,H, and Ali,K.M. “Compressive buckling of laminates with an embedded delamination”, *Composites science and technology*, 1999, 59:1247-1260
25- Riks, E., “An incremental approach to the solution of snapping and buckling problems”, *International Journal of Solids Structures*,1979, 15:529-551.